Wavefield reconstruction using wavelet transform

Iga Pawelec[1], *Paul Sava*[1] *& Michael Wakin*[2]
[1] *Center for Wave Phenomena, Colorado School of Mines*
[2] *SINE Center for Research in Signals and Networks, Colorado School of Mines*

SUMMARY

We propose wavelet-based data reconstruction to interpolate land data with large dynamic range without amplitude processing or windowing. We test two approaches using compressive sampling to recover full unaliased data: sparsity promoting reconstruction by ℓ_1 minimization and projection onto convex sets. Unlike the Fourier domain, the wavelet domain provides a good representation of non-stationary signals and allows to rebuild data of high dynamic range with relatively small percentage of all coefficients. We solve an ℓ_1 minimization problem to find a sparse representation of full data in the wavelet domain and compare it with results of a wavelet-domain POCS algorithm. Tests on field data reveal that both approaches can recover missing data highly coherent with the existing data, while taking advantage of the full dynamic range of the data.

INTRODUCTION

Modern techniques of seismic data analysis and inversion, such as AVO/AVA, full waveform inversion (FWI) and least squares reverse time migration (LSRTM), operate on big data volumes. However, multi-azimuth, long offset dense surveys are expensive to acquire and sometimes access restrictions do not permit acquisition over certain areas, resulting in data gaps. Seismic data reconstruction plays a key role in both scenarios, allowing to fill-in missing data before advanced processing and inversion are performed.

Mosher et al. (2017) show that a novel approach, utilizing ideas from compressive sensing, can significantly speed up acquisition without jeopardizing data quality. The underlying idea is to randomize receiver placement and shot timing according to compressive sampling rules and solve a large scale regularization problem, recovering a full data volume from reduced measurements. To recover full data, one must develop a strategy for dense data recovery that takes into account acquisition geometry: parameters such as source and receiver locations, maximum gap size and timing of the shots have to be considered. For example, most conventional 3D acquisition geometries have regular but poor sampling in at least one direction (Trad, 2009) and one has to contend with aliasing and sometimes big data gaps due to access restrictions. In contrast, compressive sensing surveys would have deliberate irregular sampling and often simultaneous shooting. Thus, data recovery strategy needs to be tuned with particular geometry restrictions in mind.

Current techniques for infilling missing data can be divided in several categories, including prediction error filters (PEFs) (Spitz, 1991), tensor completion (Kreimer et al., 2013), rank reduction (Chen et al., 2016) and deep learning (Wang et al., 2019). However, the most widely used interpolation techniques are transform-based approaches. Such methods are well-studied in the context of data aliasing and irregular sampling and rely on data representation in a transform domain to recover missing information. Although different transforms have been used, including Radon transform (Kabir and Verschuur, 1995; Yu et al., 2007; Wang et al., 2010) and wavelet or seislet transforms (Yu et al., 2007; Gan et al., 2015), the Fourier transform remains the most popular choice because it is easy to interpret and fast to compute. Liu and Sacchi (2004) develop a framework for data recovery based on weighted norm minimization, using spectral weights bootstrapped from FK representation of data. This framework can be extended to five dimensions (Trad, 2009). The Fourier domain is also used in the projection onto convex sets (POCS) method described by Abma and Kabir (2006). To deal with problems of non-uniform sampling and aliasing artifacts in the Fourier domain, Xu et al. (2005, 2010) propose an antileakage version of the Fourier transform. One downside of Fourier-based approaches is that data have to be windowed for non-stationarity and, as a consequence, only local information is used for interpolation. Another attractive transform for seismic data interpolation, gaining significant popularity, is the curvelet transform (Hennenfent et al., 2010; Herrmann, 2010; Naghizadeh and Sacchi, 2010). Curvelets provide an optimally sparse representation of seismic wavefields (Candès and Demanet, 2005), but their redundancy implies that for a dataset of size N, as many as $7 \times N$ curvelet coefficients have to be computed, depending on the chosen number of scales, which can be prohibitively expensive for large 3D datasets.

In this paper, we present a seismic data reconstruction strategy exploiting wavelet domain sparsity under randomized acquisition. We review the theory highlighting the favorable recovery conditions and present data reconstruction results for field data with two strategies: projection onto convex sets (POCS) and ℓ_1 norm minimization. Wavelet transform is fast to compute and represents well large dynamic range in data. The POCS approach iteratively restores missing data, but its success hinges on developing a good thresholding strategy. ℓ_1 optimization is less robust to acquisition geometry, but does not need any thresholding.

THEORY

Sparse recovery conditions

Consider an $N-$dimensional signal f which can be represented as a vector of coefficients α in some basis expansion: $f = \Phi\alpha$. f is said to be sparse if only $K \ll N$ of the coefficients α are non-zero. f is compressible when sorted coefficients α decay rapidly enough to zero, so that α can be well-approximated as sparse (Baraniuk et al., 2010).

Successful recovery of $K-$sparse or compressible signal depends on three key components: (1) the sampling strategy, (2) the sparsifying transform, and (3) the sparsity-promotion recovery. In seismic data acquisition, we acquire $d = Tm$, where d are recorded data, T is a sampling matrix and m is the full data volume needed for processing and inversion. The only freedom that can be taken in the field is where receivers are placed and when shots are fired. Thus, for seismic applications, the matrix T is sparse.

Results from compressive sensing suggest that sparse signals can be recovered without loss of information if the sampling matrix satisfies the so called *restricted isometry property* (RIP) (Baraniuk, 2007). RIP is satisfied with high probability for Gaussian and sub-Gaussian matrices or when sampling non-uniformly Fourier-sparse signals. Then, the number of measurements to recover K-sparse signal is $M = O(K \log(N/K))$. However, this results may not hold for non-uniform sampling in other domains.

Let $m = \Phi^T\alpha$ and $d = T\Phi^T\alpha$, where α represents the signal in the sparse domain. In this scenario, the RIP is satisfied if Φ is a Fourier transform and the sparsity promoting recovery can be achieved by solving the following ℓ_1 optimization problem:

$$\tilde{\alpha} = \arg\min_{\alpha} \|\alpha\|_1 \text{ subject to } d = T\Phi^T\alpha. \qquad (1)$$

However, for other transforms (such as the wavelet transform or the curvelet transform), there is no practical algorithm to compute RIP constants (Herrmann, 2010) and provide similar recovery guarantees. A way to gain an insight into recovery behavior of a given sampling matrix - transform pair, one can construct a phase transition diagram. For different realizations of a $K-$sparse signal, one computes the chance of successful recovery by looking at the difference between original and recovered signal. Figure 1 shows such a diagram for 1D wavelet domain $K-$sparse signal with a binary sampling matrix (data are a subset of true wavelet coefficients). Note that for successful recovery in this scenario, one needs a relatively high number of measurements.

Sampling patterns in the wavelet domain

Hennenfent and Herrmann (2008) present a detailed analysis of sampling patterns in the frequency domain and show that signals can be recovered well when sampling artifacts, known as spectral leakage, do not have a sparse

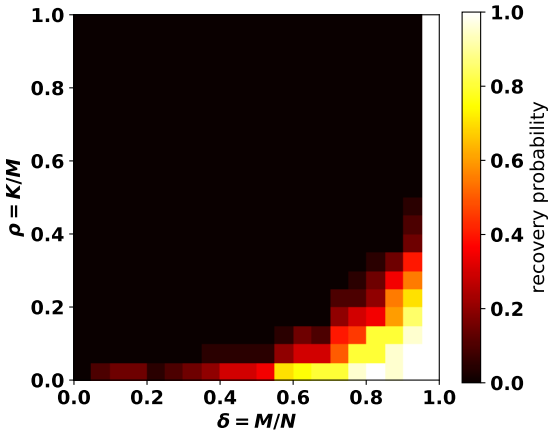

Figure 1: Phase transition diagram for sparse sampling matrix and wavelet domain sparse data. N is the signal length, K is the sparsity, and M is the number of measurements.

representation in the frequency domain. Regular undersampling results in aliases at particular frequencies. In contrast, irregular (random) downsampling results in white noise-like spectral leakage. Therefore, random downsampling yields much more favorable recovery conditions. The question is, however, whether these results hold for other Fourier-related domains?

Figure 2 shows uniform and random downsampling of the seismic trace and the resulting wavelet coefficients. Note that signal aliases appear at scales -2 and -3 for the uniform downsampling, whereas for random downsampling, noisy images appear at all scales. This is a consequence of the implementation of the digital wavelet transform with a filter bank, as described in Mallat (1999).

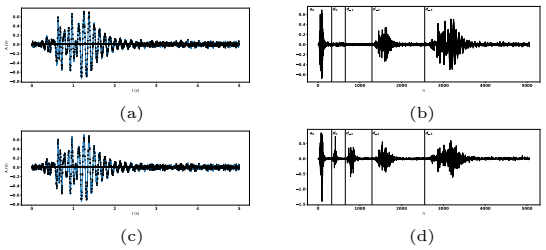

Figure 2: Different undersampling strategies and their imprint in the wavelet domain. (a) Regular downsampling by a factor of 4, (c) random downsampling by the same factor. (b), (d): Wavelet coefficients for strategies shown in (a), (c), respectively.

Projection onto convex sets

Another method of data reconstruction, which does not rely on sparsity explicitly, is projection onto convex sets (POCS). It this method, the data to be recovered are assumed to have some known properties (such as being

band-limited). We also assume that: (1) all signals are members of a Hilbert space $\mathcal{H}$, (2) signals with desired properties lie in subsets of $\mathcal{H}$, and (3) subsets describing properties are *closed linear manifolds*. Let $\mathcal{P}$ be a closed linear manifold in a Hilbert space that represents the desired property and let P be orthogonal projection operator onto $\mathcal{P}$. Suppose the recorded singnal $f \in \mathcal{H}$. Then the signal with desired properties g is the unique projection $Pf = g \in \mathcal{P}$ that is closest to f in some appropriate norm (Moon and Stirling, 2000). We solve an optimization problem of the form

$$\min_{g \in \mathcal{P}} \mathcal{J} = \|f - g\|, \tag{2}$$

by the method of alternating projections (Moon and Stirling, 2000).

Abma and Kabir (2006) introduce the application of POCS to seismic data reconstruction by alternating projections in the $F-K$ domain. Their idea is to transform data with gaps to the $F-K$ domain, project back with only a few biggest coefficients, re-inject original data and repeat the process, while progressively lowering the threshold applied to the coeficients in the transform domain. The challenge lies in deciding on a thresholding strategy. Starting from just a few highest coefficients may lead to undesirable results for signals with large dynamic range (recall Figure **??**). Therefore, the choice of transform and knowledge about signal properties in the transform domain is of key importance for the success of this strategy.

We show that POCS can successfuly recover missing data with large dynamic range if the wavelet transform is used instead of the $F-K$ transform. Wavelets reconstruct large-dynamic range signals starting from the high-energy portion of signals; progressive lowering of the threshold allows to accurately reconstruct weaker portions of signals. We find that logarithmic thresholding, starting from 0.1% of largest coefficients and relaxing the threshold values to 20% of the highest coefficients yields satisfactory results. To achieve similar results in the $F-K$ domain, windowing or amplitude processing would be required.

FIELD DATA EXAMPLE

We demonstrate data reconstruction for data with large dynamic range using two wavelet domain approaches: sparsity promoting ℓ_1 optimization problem described in equation 1 and the POCS approach described in equation 2. In the first case, we use the Spectral Projected Gradient solver (Van Den Berg and Friedlander, 2008). For POCS, we follow the scheme proposed by Abma and Kabir (2006), while replacing the Fourier transform with a wavelet transform. We use logarithmic thresholding applied to all scales except the coarse scale, which we leave unchanged.

We demonstrate data reconstruction example designed for compressive seismic acquisition, following the jittered undersampling strategy described by Hennenfent and Herrmann (2008). The field data example showcases land data with large dynamic range, strong and slow surface waves, and weaker seismic signals. The input for the reconstruction algorithms are unwindowed, unprocessed data. The field data example uses an unprocessed shot from a dense 2D land survey conducted by Colorado School of Mines in Pagosa Springs, Colorado. Regular downsampling by a factor of 2 would introduce aliasing, so instead we follow the jittered undersampling approach of Hennenfent and Herrmann (2008). Figure 3a shows the selected shot; the data are clipped for display but reconstruction is run on the raw shot, without windowing or amplitude balancing.

To quantify the quality of the reconstruction, we use signal-to-noise ratio, defined as:

$$SNR = 20 \log_{10} \Big(\frac{\|x\|}{\|x - \hat{x}\|} \Big), \tag{3}$$

where x represents original full data and $\hat{x}$ represents reconstructed data. We also look at the coherence between full and recovered data, computed separately for every trace as a measure of similarity between original and reconstructed data, and the difference image.

The reconstructed data are shown in Figure 4. The most noticeable differences between full and reconstructed data are in the immediate vicinity of the source. The signal-to-noise ratio is higher for ℓ_1 recovery at 7.0dB compared to 4.3dB for POCS. Examining the wavelet spectra in Figure 5 shows that ℓ_1 reconstruction yields a sparser spectrum than that of the original data, while POCS reconstruction increases the strength of some coefficients compared to the original data. This observation can explain the higher SNR for sparse reconstruction. The trace coherence in both cases is close to 1. Looking at the difference images reveals that reconstruction mostly distorts the high amplitude jumps. This phenomenon is related to the wavelet spectra of reconstructed data and to the limited directional sensitivity of the 2D wavelet transform.

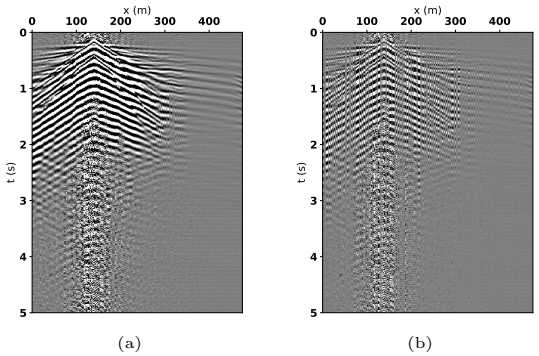

Figure 3: (a) Field data used in reconstruction tests, and (b) the data with 50% missing traces.

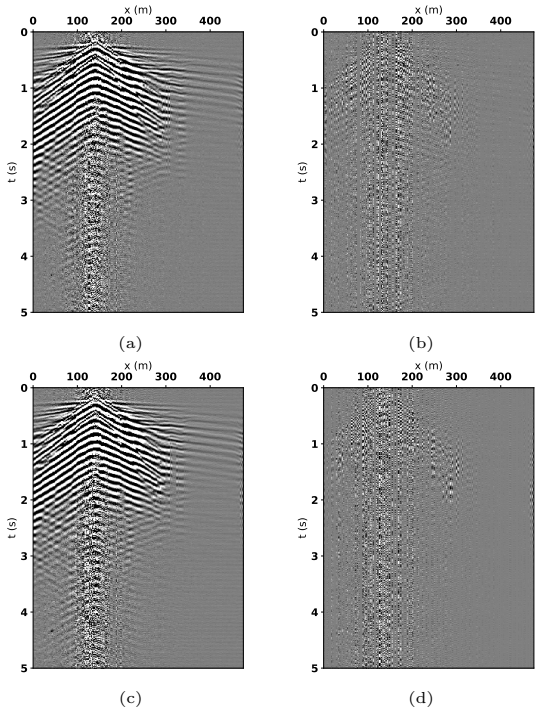

Figure 4: Field data reconstruction results for (a) ℓ_1 optimization and (c) POCS. (b) and (d) are the corresponding data differences with respect to the full data in Figure 3a. Both reconstructions struggle in the similar way with high frequency details, but the sparsity promoting approach has higher SNR.

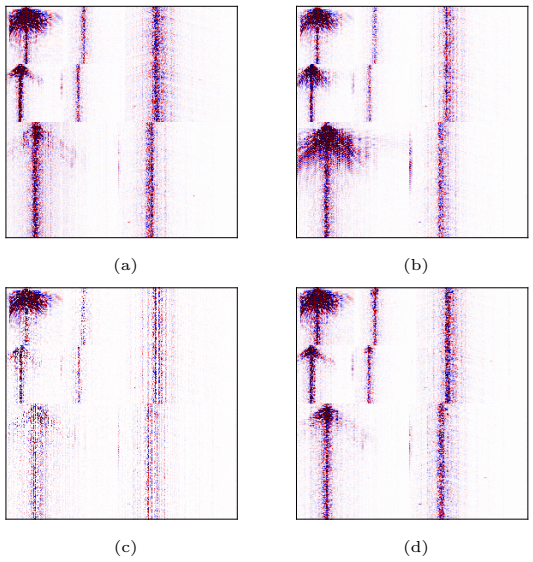

Figure 5: Wavelet spectra of (a) the full field data, (b) downsampled data, data reconstructed with (c) ℓ_1 optimization and (d) with POCS. Note that ℓ_1 reconstruction yields a sparser wavelet spectrum than POCS.

DISCUSSION AND CONCLUSIONS

Acquisition of dense unaliased data on land is an expensive undertaking. Our data wavelet-based reconstruction results are a first step towards designing acquisition geometry which uses fewer sensors and allows recovery of full data without the need for amplitude processing or windowing. Non-aliased surface waves can provide a wealth of information about the shallow subsurface, potentially helping to solve near-surface challenges, such as building shallow velocity models and correctly accounting for strong shallow heterogeneity (Keho and Kelamis, 2012). However, further refinements in data reconstruction are needed to achieve even higher reduction in channel count: the average receiver spacing in our scenario is 2.5m, while practical average spacing would be on the order of 10m or more.

We demonstrate that both ℓ_1 sparsity promoting optimization and POCS can be used to recover seismic data with large dynamic range in the wavelet domain. The main advantage of using the wavelet domain is that it allows to avoid data windowing and the computations are faster than for the Fourier transform.

Our reconstruction strategies are kinematically correct for strong and weak events alike. The relative amplitude ratio is also preserved. Observable differences between true and recovered data are primarily confined to the high amplitude events. This allows to use reconstructed data to analyze and remove surface wave, without jeopardizing much weaker reflection signals.

The wavelet transform in 2D is limited to three orientations (horizontal, vertical and diagonal), and therefore, representation of edges at different angles is suboptimal, and thus the sparsity promoting approach misses detail. In that regard curvelets have a distinct advantage if one can afford to store all coefficients of the transformation.

ACKNOWLEDGEMENTS

We would like to acknowledge Dawson and Sercel for providing equipment and technical support at the CSM Geophysical Field Camp. We extend our thanks to GTI for allowing us to test wireless nodes and conduct dense sampling experiments. SEG provided partial financial support of the Field Camp. We also acknowledge the CSM undergraduate students who conducted the field data acquisition.

REFERENCES

Abma, R., and N. Kabir, 2006, 3D interpolation of irregular data with a POCS algorithm: Geophysics, **71**, E91–E97.

Baraniuk, R. G., 2007, Compressive sensing [lecture notes]: IEEE Signal Processing Magazine, **24**, 118–121.

Baraniuk, R. G., V. Cevher, M. F. Duarte, and C. Hegde, 2010, Model-based compressive sensing: IEEE Transactions on Information Theory, **56**, 1982–2001.

Candès, E. J., and L. Demanet, 2005, The curvelet representation of wave propagators is optimally sparse: Communications on Pure and Applied Mathematics, **58**, 1472–1528.

Chen, Y., D. Zhang, S. Zu, S. Gan, W. Huang, X. Chen, and Z. Jin, 2016, Simultaneous denoising and reconstruction of 5-D seismic data via damped rank-reduction method: Geophysical Journal International, **206**, 1695–1717.

Gan, S., S. Wang, Y. Chen, Y. Zhang, and Z. Jin, 2015, Dealiased seismic data interpolation using seislet transform with low-frequency constraint: IEEE Geoscience and remote sensing letters, **12**, 2150–2154.

Hennenfent, G., L. Fenelon, and F. J. Herrmann, 2010, Nonequispaced curvelet transform for seismic data reconstruction: A sparsity-promoting approach: Geophysics, **75**, WB203–WB210.

Hennenfent, G., and F. J. Herrmann, 2008, Simply denoise: Wavefield reconstruction via jittered undersampling: Geophysics, **73**, V19–V28.

Herrmann, F. J., 2010, Randomized sampling and sparsity: Getting more information from fewer samples: Geophysics, **75**, WB173–WB187.

Kabir, M. N., and D. Verschuur, 1995, Restoration of missing offsets by parabolic Radon transform: Geophysical Prospecting, **43**, 347–368.

Keho, T. H., and P. G. Kelamis, 2012, Focus on land seismic technology: The near-surface challenge: The Leading Edge, **31**, 62–68.

Kreimer, N., A. Stanton, and M. D. Sacchi, 2013, Tensor completion based on nuclear norm minimization for 5D seismic data reconstruction: Geophysics, **78**, V273–V284.

Liu, B., and M. D. Sacchi, 2004, Minimum weighted norm interpolation of seismic records: Geophysics, **69**, 1560–1568.

Mallat, S., 1999, A wavelet tour of signal processing: Elsevier.

Moon, T. K., and W. C. Stirling, 2000, Mathematical methods and algorithms for signal processing: Prentice Hall Upper Saddle River, NJ, **1**.

Mosher, C. C., C. Li, F. D. Janiszewski, L. S. Williams, T. C. Carey, and Y. Ji, 2017, Operational deployment of compressive sensing systems for seismic data acquisition: The Leading Edge, **36**, 661–669.

Naghizadeh, M., and M. D. Sacchi, 2010, Beyond alias hierarchical scale curvelet interpolation of regularly and irregularly sampled seismic data: Geophysics, **75**, WB189–WB202.

Spitz, S., 1991, Seismic trace interpolation in the f-x domain: Geophysics, **56**, 785–794.

Trad, D., 2009, Five-dimensional interpolation: Recovering from acquisition constraints: Geophysics, **74**, V123–V132.

Van Den Berg, E., and M. P. Friedlander, 2008, Probing the Pareto frontier for basis pursuit solutions: SIAM Journal on Scientific Computing, **31**, 890–912.

Wang, B., N. Zhang, W. Lu, and J. Wang, 2019, Deep-learning-based seismic data interpolation: a preliminary result: Geophysics, **84**, V11–V20.

Wang, J., M. Ng, and M. Perz, 2010, Seismic data interpolation by greedy local Radon transform: Geophysics, **75**, WB225–WB234.

Xu, S., Y. Zhang, and G. Lambaré, 2010, Antileakage Fourier transform for seismic data regularization in higher dimensions: Geophysics, **75**, WB113–WB120.

Xu, S., Y. Zhang, D. Pham, and G. Lambaré, 2005, Antileakage Fourier transform for seismic data regularization: Geophysics, **70**, V87–V95.

Yu, Z., J. Ferguson, G. McMechan, and P. Anno, 2007, Wavelet-Radon domain dealiasing and interpolation of seismic data: Geophysics, **72**, V41–V49.